Appl. Phys. B 32, 79–81 (1983)

Applied Physics B Photophysics and Laser Chemistry

cw Far-Infrared Lasing in $^{15}NH_3$, Stark Resonantly Pumped by a CO_2 or N_2O Laser

C. Gastaud, P. Belland, M. Redon, and M. Fourrier

Université Pierre et Marie Curie, Laboratoire de Dispositifs Infra-Rouge, Tour 12, 4 place Jussieu, F-75230 Paris Cedex 05, France

Received 24 June 1983/Accepted 1 July 1983

Abstract. 48 new resonant pumping schemes, by ir Stark tuning, have been performed on $^{15}NH_3$, with cw CO_2 and N_2O lasers. Among the 25 different fir wavelengths obtained, 15 correspond to new emissions, raising thus to 45 the total number of cw fir emissions from this gas, in the presence of electric field.

PACS: 33, 42.55

In a previous paper [1], we reported 30 new cw far-infrared (fir) lasing lines in $^{15}NH_3$ optically pumped by a CO_2 or a N_2O laser.

The Stark tuning of the infrared (ir) transition frequencies to those of the pumping radiations can be correctly achieved if the Stark ir spectrum has been investigated before any attempt for fir lasing experiment is made. Our preliminary fir lasing research is based on the identification in Stark ir spectroscopy by Shimizu [2], but we then observed fir laser actions for electric fields not given by Shimizu, due to other ir coincidences.

We have thus systematically reinvestigated the Stark ir spectrum with all the lines of the CO_2 and the N_2O lasers, for electric fields varying from 0 to 70 kV/cm. We have made the identifications of the ir transitions by means of the data of Shimoda et al. [3] and in some cases, due to the fir emissions.

The Stark fir laser and the pump laser have already been described [4]. The Stark field applied to the gas can be parallel to the electric field of the linearly polarized pumping radiation ($\Delta M=0$) or perpendicular to it ($\Delta M=\pm 1$).

The experimental results are reported in Table 1. The wavelengths were measured with an accuracy of $\pm 0.3\%$ by means of a Perot-Fabry interferometer fitted with meshes. The calculation of the fir wavelengths have been made with the molecular constants of [3]. The fir transitions, named according to absorption rules, belong to the $v_2=1$ state of the v_2 vibration.

The pump-laser lines belong to the CO_2 laser if they are prefixed with 9 or 10 and to the N_2O laser otherwise. The $10R(3)$ line is a sequential one, lasing without any special arrangement in the CO_2 laser cavity. The Stark frequency shifts (higher than 26 GHz in some cases) appearing in the 6th column, are calculated, up to the second order, by means of the molecular constants of [3] and the inversion energies of the $v_2=0$ state come from the spectral constants of Sasada [5].

The Stark-field values correspond to the first M component (lower Stark field) giving rise to fir laser action, generally the $M=J$ component and for a $\Delta M=0$ pumping. When M is lower than J, its value is specified. If no laser action occured for the $\Delta M=0$ pumping, but only at $\Delta M=\pm 1$, the subscript $\perp$ is attached the value of the electric field. The accuracy of this Stark field is estimated to be $\pm 0.1\%$ for values lower than 50 kV/cm and $\pm 0.8\%$ for higher values.

The polarization of the emitted fir radiation, checked with a grid analyser, is reported in the 8th column: $\parallel$ (or $\perp$) means that the electric field of the fir radiation is parallel (or perpendicular) to the metal walls of the hybrid metal dielectric waveguide. When no polarization appears, it comes from the fact that the wavelength is too short compared to the 50 μm wire spacing of our grids.

Table 1. New pumping schemes in $^{15}NH_3$ (see text). (a) $M=4$, (b) $M=6$

λ measured [μm]	λ calculated [μm]	fir transition	ir laser line	ir transition	Shift [GHz] $\nu_{NH_3}-\nu_{pump}$	Electric field [kV/cm]	fir polarization	Relative strength
318.69	317.82	*saQ*(5, 3)	9*P*(4)	*saR*(4, 3)	−11.03	42.47	⊥ or ∥	*W*⊥
317.04	317.82	*saQ*(5, 3)	9*P*(6)	*aaR*(4, 3)	15.97	55.90	⊥	*W*⊥
302.64	302.21	*saQ*(5, 4)	9*P*(4)	*saR*(4, 4)	−12.28	35.03	⊥ or ∥	*W*⊥
301.50	302.21	*saQ*(5, 4)	9*P*(6)	*aaR*(4, 4)	13.44	37.87⊥	⊥	*W*⊥
302.77	301.80	*saQ*(4, 3)	9*P*(28)	*aaR*(3, 3)	26.35	65.77	⊥	*W*⊥
301.93	301.80	*saQ*(4, 3)	10*P*(36)	*asQ*(5, 3)	3.18	23.13	⊥ or ∥	M∥
298.90	301.80	*saQ*(4, 3)	*R*(29)	*saQ*(4, 3)	−16.81	56.17	∥	*M*⊥
302.13	301.40	*saQ*(6, 5)	10*P*(2)	*aaQ*(6, 5)	7.12	41.33(a)	∥	*W*⊥
301.38	301.40	*saQ*(6, 5)	*R*(25)	*aaQ*(6, 5)	8.50	46.27(a)	⊥ or ∥	*W*⊥
301.03	299.40	*saQ*(7, 6)	*R*(26)	*saQ*(7, 6)	−18.66	56.80(b)⊥	∥	*W*⊥
292.69	291.30	*saQ*(1, 1)	10*R*(8)	*asR*(1, 1)	4.89	31.63	∥	*M*⊥
291.88	291.30	*saQ*(1, 1)	10*R*(2)	*saQ*(1, 1)	−15.24	63.13	∥	*M*⊥
291.87	291.30	*saQ*(1, 1)	*R*(30)	*saQ*(1, 1)	− 7.86	41.00	∥	*M*⊥
291.21	291.03	*saQ*(2, 2)	*R*(30)	*saQ*(2, 2)	−15.02	47.37	∥	*S*⊥
290.83	291.03	*saQ*(2, 2)	*R*(28)	*aaQ*(2, 2)	6.11	27.33	∥	*M*⊥
290.33	291.03	*saQ*(2, 2)	10*R*(3)	*aaQ*(2, 2)	5.51	25.67	⊥ or ∥	*M*⊥
290.30	289.60	*saQ*(3, 3)	*R*(27)	*aaQ*(3, 3)	16.27	46.50	⊥ or ∥	*S*⊥
289.23	289.60	*saQ*(3, 3)	*R*(30)	*saQ*(3, 3)	−26.76	64.07	⊥ or ∥	*M*⊥
288.00	287.02	*saQ*(4, 4)	*R*(27)	*aaQ*(4, 4)	0.22	3.87	⊥	*M*∥
286.45	287.02	*saQ*(4, 4)	*R*(26)	*aaQ*(4, 4)	22.34	55.33	∥	*W*⊥
285.33	287.02	*saQ*(4, 4)	*R*(29)	*saQ*(4, 4)	−20.75	50.00	⊥ or ∥	*W*⊥
283.33	283.35	*saQ*(5, 5)	10*R*(3)	*saQ*(5, 5)	−19.25	45.73	⊥	*W*⊥
282.50	283.35	*saQ*(5, 5)	*R*(28)	*saQ*(5, 5)	−18.62	44.67	⊥	*W*∥
273.03	272.93	*saQ*(7, 7)	10*P*(2)	*saQ*(7, 7)	− 5.33	19.40	⊥	*W*∥
272.73	272.93	*saQ*(7, 7)	*R*(25)	*saQ*(7, 7)	− 4.03	28.90(a)	∥	*W*⊥
259.00	258.96	*saQ*(9, 9)	*R*(22)	*saQ*(9, 9)	− 4.36	17.33	⊥	*W*∥
149.43	149.24	*asR*(4, 3)	9*P*(38)	*ssR*(4, 3)	−21.07	68.33	∥	*S*⊥
148.80	149.24	*asR*(4, 3)	*P*(12)	*asQ*(5, 3)	15.22	61.77	∥	*S*∥
93.80	93.63	*asR*(6, 5)	9*R*(2)	*asR*(6, 5)	11.87	37.50⊥	∥	*W*⊥
88.18	88.18	*saR*(3, 3)	*R*(29)	*saQ*(4, 3)	−16.81	56.17	∥	*S*∥
88.07	88.18	*saR*(3, 3)	9*P*(28)	*aaR*(3, 3)	26.35	65.77	∥	*S*⊥
76.91	76.80	*asR*(7, 4)	9*R*(38)	*asR*(7, 4)	16.43	63.60	∥	*W*⊥
76.72	76.70	*saR*(4, 2)	9*P*(4)	*saR*(4, 2)	− 9.64	57.23	∥	*M*∥
76.67	76.70	*saR*(4, 2)	10*R*(3)	*saQ*(5, 2)	− 5.93	48.93	∥	*W*∥
75.85	75.98	*saR*(4, 3)	10*R*(3)	*saQ*(5, 3)	− 9.58	45.00	∥	*W*∥
75.83	75.98	*saR*(4, 3)	*R*(26)	*aaQ*(5, 3)	14.92	63.33	∥	*W*∥
75.72	75.98	*saR*(4, 3)	9*P*(6)	*aaR*(4, 3)	15.97	55.90	∥	*M*∥
67.33	67.45	*saR*(5, 2)	*R*(26)	*aaQ*(6, 2)	5.52	54.53	∥	*W*∥
67.00	66.91	*saR*(5, 3)	*R*(26)	*aaQ*(6, 3)	0.62	11.00	∥	*W*∥
66.15	66.16	*saR*(5, 4)	9*R*(22)	*saR*(5, 4)	−19.65	57.10⊥	∥	*W*⊥
59.88	59.90	*saR*(6, 3)	10*P*(2)	*aaQ*(7, 3)	5.77	41.90	—	*W*∥
59.85	59.90	*saR*(6, 3)	*R*(25)	*aaQ*(7, 3)	7.11	47.93	∥	*M*∥
53.96	53.84	*saR*(7, 4)	10*P*(2)	*saQ*(8, 4)	− 1.96	18.03	—	*W*∥
53.88	53.84	*saR*(7, 4)	*R*(25)	*saQ*(8, 4)	− 0.59	9.50	—	*W*∥
52.52	52.46	*saR*(7, 6)	10*P*(4)	*aaQ*(8, 6)	8.65	32.27	—	*W*∥
52.51	52.46	*saR*(7, 6)	10*P*(2)	*saQ*(8, 6)	−19.42	54.70	—	*W*∥
52.47	52.46	*saR*(7, 6)	*R*(23)	*aaQ*(8, 6)	7.09	28.37	—	*W*∥
48.25	48.27	*saR*(8, 6)	*R*(22)	*aaQ*(9, 6)	9.92	37.77	—	*W*∥

It is well known that, for a rectangular hybrid metal dielectric waveguide, the low-loss modes of propagation have the E-field polarization parallel to the metal walls [6], thus explaining why the fir polarization has always been observed to be parallel, irrespective of the pump electric-field polarization.

On Fig. 1, the loss coefficient $\alpha_{\parallel}$ (or $\alpha_{\perp}$) of the lowest-order mode of propagation for the E-field parallel (or perpendicular) to the metal walls has been plotted versus wavelength, for a $3\times15\,\mathrm{mm}^2$ cross-section of the waveguide, 3 mm being the spacing between the aluminium walls and 15 mm the width between the plexiglas walls. As one can see from this figure, the ratio $\alpha_{\perp}/\alpha_{\parallel}$ decreases as the wavelength increases; thus, for long wavelengths, the direction of the fir polarization might be no longer imposed by the waveguide but the pump polarization, via the matrix elements of the dipole electric moments μ, of the ir and fir transitions.

We have experimentally observed that in some cases, for wavelengths longer than typically 250 µm, the polarization of the fir E-field could be perpendicular to the metal walls. These long wavelengths are the more often associated with Q-fir transitions (inversion transitions) for which the matrix elements of a $\Delta M=0$ transition (E_{fir} $\perp$ to the metal walls) ($\mu^2 \sim 4M^2$) are higher than those for a $\Delta M=\pm 1$ transition (E_{fir} $\parallel$ to the metal walls) $[\mu^2 \sim (J\pm M)(J\mp M+1)]$, for values of M close to the value of J. Thus, although the propagation losses increase for longer wavelengths, the high gain of the ammonia laser still permits oscillation for these long wavelengths with polarization imposed by the quantum numbers and no longer by the waveguide structure. The M dependence of these matrix elements is such that for M decreasing from J to 1, the dipole matrix element of the fir $\Delta M=\pm 1$ transition increases while the one of the $\Delta M=0$ transition decreases, implying thus a rotation of the polarization; this rotation has been experimentally observed in all the cases for which the polarization is at first perpendicular, for $M=J$.

The powers given in the last column have been estimated by means a Scientech power meter 3610, in each case for the maximum possible pressure (minimum 40 mTorr) compatible with the breakdown voltage; the selection rules of the pump are specified by $\parallel$ for $\Delta M=0$ and $\perp$ for $\Delta M=\pm 1$. The indicated powers are: W for a power lower than 0.1 mW; M for a power between 0.1 mW and 1 mW; S for a power higher than 1 mW.

In conclusion, the number of Stark fir emissions has been increased from 30 to 45. The wavelength values of two transitions of the same name, one belonging to $^{15}NH_3$ and the other to $^{14}NH_3$ are

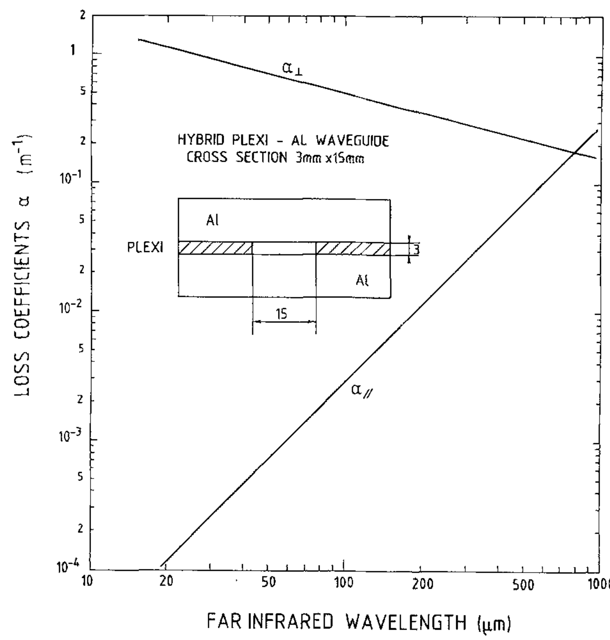

Fig. 1. Loss coefficients $\alpha_{\parallel}$ and $\alpha_{\perp}$ vs. the fir wavelength for a $3\times 15\,mm^2$ hybrid metal dielectric waveguide cross-section

significantly different and the Stark fir emission spectra of $^{15}NH_3$ and $^{14}NH_3$ are complementary to one another, with more than 110 lines.

References

1. C. Gastaud, A. Sentz, M. Redon, M. Fourrier: Opt. Lett. **6**, 449–451 (1981)
2. F. Shimizu: J. Chem. Phys. **53**, 1149–1151 (1970)
3. K. Shimoda, Y. Ueda, J. Iwahori: Appl. Phys. **21**, 181–189 (1980)
4. M. Redon: «Nouvelles raies d'émission, en régime continu, d'un laser submillimétrique à ammoniac pompé, en présence d'effet Stark intense, par laser à CO_2 ou à N_2O». Thesis, University of Paris (1980)
5. H. Sasada: J. Mol. Spectrosc. **83**, 15–20 (1980)
6. M.S. Tobin, R.E. Jensen: Appl. Opt. **15**, 2023–2024 (1976)